Negatively thermodynamic toughening in double network hydrogel towards cooling-triggered multi-shape memory effect

Haibao Lu[a,*], Zhenghong Li[a], Xiaodong Wang[a], Ziyu Xing[a] and Yong Qing Fu[b,*]

[a]National Key Laboratory of Science and Technology on Advanced Composites in Special Environments, Harbin Institute of Technology, Harbin 150080, China

[b]Faculty of Engineering and Environment, Northumbria University, Newcastle upon Tyne, NE1 8ST, UK

[*]Corresponding author, E-mail: luhb@hit.edu.cn and richard.fu@northumbria.ac.uk

Abstract: This paper explores fundamental mechanisms of negatively thermodynamic toughening during microphase separations of double network (DN) hydrogels, which have dynamically coordinating components with adjustable swelling behavior and designable multi-shape memory effect (multi-SME). Based on the Flory-Huggins theory and Fick's second law, a thermodynamic model is formulated to study the diffusive dynamics, cooling-triggered multi-SME and mechanical toughness of the DN hydrogels. The negatively thermodynamic toughening effect of the DN hydrogels is strongly dependent on their water concentration, hydrophobic transition and microphase separation. Finally, effectiveness of this new model is demonstrated by applying it to predict dual-SME, quadruple-SME and cooling-triggered shape memory behaviors of DN hydrogels. This study provides a methodology for the design of shape memory DN hydrogels with tunable, giant and programmable cooling-triggered multi-SME.

Keywords: shape memory effect; hydrogel; double network; thermodynamics

1. Introduction

Shape memory polymers (SMPs) are stimulus-responsive materials which possess excellent properties including large recovery strain, low cost and biocompatibility [1-6]. Owing to the entropic elasticity of their macromolecular chains, SMPs can recover their original shapes from the pre-defined temporary shapes, by means of direct and inductive heating stimuli [7,8]. One of the most popular types of SMPs is composed of hard and soft segments [9]. The hard segment plays a critical role to memorize the permanent shape and orientations of macromolecules, whereas the soft one responds to the external stimulus and generates a transition from a "frozen" state to an active one [10,11]. The macromolecular chains which are composed of both the hard and soft segments could retain the permanent shape from their temporary ones, therefore generating the shape memory effect (SME).

Cooling-triggered SME was first reported in the shape memory hybrid, which was made of a plastic sponge (as an elastic component) filled with poloxamer gel (as a transition component) [12]. Recently, double network (DN) hydrogel has been developed, using a network of poly-acrylamide (PAAm) and methylcellulose (MC). The PAAm network acts as the hard component to store the entropic energy, and the MC network acts as the soft component to fix a temporary shape through the reversibly hydrophobic crosslinks in response to an external stimulus [13]. The hydrophobic methoxy groups in the MC network ensure its solubility in cold water and formation of gelation upon heating [14,15], as shown in Figure 1. Here, we define two temperature limits, e.g., high temperature limit and the low temperature limit. As

the temperature reaches the high temperature limit, the hydrophobic interaction in MC networks is significant, while PAAm and MC networks are formed inside the macromolecules. On the other hand, the hydrophobic interaction is weakened when the ambient temperature is decreased to the low temperature limit. Therefore, water molecules form clathrates around the hydrophobic methoxy groups of MC network, which result in hydration and entanglement due to entropy-driven assembly of clathrates [16].

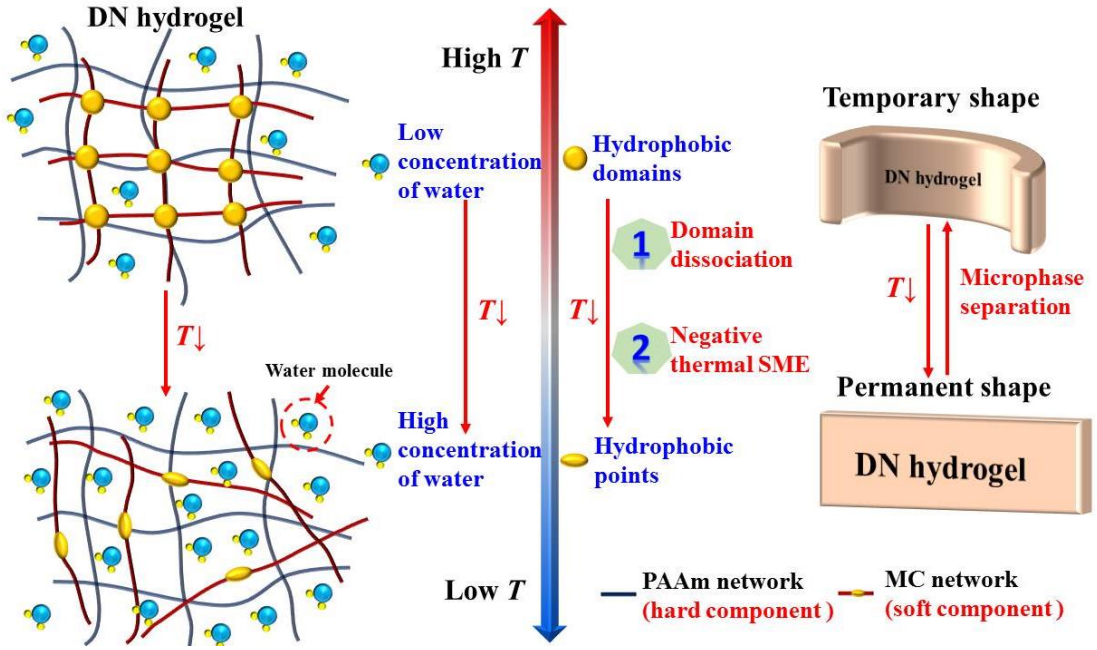

Figure 1. Illustration of negatively thermodynamic toughening and cooling-triggered SME of PAAm-MC DN hydrogel, as a function of temperature.

Meanwhile, other types of soft chains can be supported by reversible crosslinks of hydrogen bonding, ionic assembly and dipole-dipole generated by thermal transitions of crystallization [17-19]. The permanent shape of the DN hydrogel can be recovered during cooling process, thus generating a cooling-triggered SME due to the hydrophobic transitions and subsequent dissociations of the clathrates. Most polymers

become soft and their moduli decrease with an increase in the temperature (e.g., above either their glass transition or the melting transition temperatures). However, the negatively thermodynamic toughening effect of DN hydrogels results in an abnormal response to temperature, their thermomechanical moduli increase with the increase of temperature. Therefore, this effect enables the shape memory hydrogels to achieve a higher mechanical strength at a higher temperature. The cooling-triggered shape recovery behavior not only provides a viable actuator for biomedical applications, but also enables novel applications at a low temperature or in cold weather [20].

To understand effects of fluid permeation on the deformation behavior of hydrogels, Chester et. al. proposed a coupled theory which considers both fluid permeation and large deformation behavior of hydrogels [21]. They further substituted this theory into the finite element software to study the fluid permeation effect on the properties of thermally responsive gels [22,23]. Numerous models have been developed to understand the toughening mechanism and Mullins effect in DN hydrogels [24-27]. However, few theoretical studies have been done for this uniquely cooling-triggered shape memory DN hydrogels due to the scaling relationship between molecular structures and macroscopic properties. Such research could provide fundamental principle for the design of shape memory DN hydrogels with tunable, giant and programmable shape recovery.

In this study, the Flory-Huggins theory [28,29] is firstly employed to characterize the thermodynamics of cooling-triggered shape memory behaviors and negatively thermodynamic toughening in shape memory DN hydrogels. By combining the Fick's

second law [30,31], a diffusive dynamic model is formulated for the microphase separation and subsequent hydrophobic dissociation of soft component. The Obukhov model [32] is then employed to construct the constitutive relationship of multi-SMEs and their dynamic shape memory behaviors. The relationship between stress and strain has been formulated to explore the toughening mechanism and predict the mechanical behaviors of the DN hydrogels. Finally, the newly proposed models are validated using the experimental results of the dual-, quadruple-shape recovery and dynamic mechanical behaviors of the DN hydrogels reported in literature.

2. Modelling of cooling-triggered SME

As reported in Ref. [13], the PAAm-MC DN hydrogel shows a cooling-triggered SME owing to the hydrophobic transition of their MC component. The transition dynamics is originated from the microphase separation between the PAAm and MC components to form PAAm-water and MC-water phases. Based on the Flory-Huggins theory [28,29], the equilibrium chemical potentials of those two phases are,

$$V_{PW}\Delta\mu_{PW} = V_{MW}\Delta\mu_{MW} \tag{1}$$

where V_{PW} and V_{MW} are the volume concentrations of PAAm-water and MC-water phases, respectively, $\Delta\mu_{PW}$ and $\Delta\mu_{MW}$ are the chemical potentials of PAAM-water and MC-water phases, respectively. $\Delta\mu_{PW}$ can also be derived as [28],

$$\Delta\mu_{PW} = RT\alpha\phi_s / M_{PW} + RTA_2\alpha^2\phi_s^2 \tag{2}$$

where R is the gas constant, T is the temperature, α is the concentration coefficient, ϕ_s is the volume concentration of water in hydrogel, M_{PW} is the molar weight of PAAm-water phase and A_2 is the second virial coefficient [28].

According to equation (1), the volume concentration of water in MC-water phase (ϕ_f) can be obtained as [33],

$$\phi_f = \frac{V_{MW}}{V_{MW}+V_{PW}} = \frac{1}{1+\Delta\mu_{MW}/\Delta\mu_{PW}} \tag{3}$$

Substituting equation (2) into (1), the ϕ_f can be written as,

$$\phi_f = \frac{1}{1+\Delta\mu_{MW}/(RT\alpha\phi_s/M_{PW}+RTA_2\alpha^2\phi_s^2)} \tag{4}$$

On the other hand, to predict the dynamic behavior of DN hydrogel, the effect of diffusion time (t) on the volume concentration of water in hydrogel (ϕ_s) should be considered. As it is well known, Fick's second law is used to characterize the diffusive dynamics of a diffusion process [30,31]. The equilibrium water concentration ($\bar{C}(t)$) is introduced to describe the diffusion as following [30],

$$\bar{C}(t) = \frac{8}{\pi^2}\exp\left(-\frac{t\pi^2 D}{h^2}\right)(C_0 - C_f) + C_f \tag{5}$$

where C_0 is the initial water concentration, D is the diffusion coefficient, h is the diffusion length and C_f is the hole saturation constant in the polymer.

Based on the quasi-lattice theory [34], each water molecule occupies one lattice, and each polymer occupies m connected lattices. The dynamic relationship between the volume concentration of the water ($\phi_s(t)$) and the equilibrium water concentration ($\bar{C}(t)$) can be described using [34],

$$\bar{C}(t) = \frac{n_s}{V} = \frac{n_s}{v_m \cdot n_m + v_s \cdot n_s} \tag{6-a}$$

$$\phi_s(t) = \frac{v_s n_s}{v_m \cdot n_m + v_s \cdot n_s} \tag{6-b}$$

where V is the volume of shape memory DN hydrogels. n_s and n_m are the molar

numbers of water and gel, respectively. v_s and v_m are the molar volumes of water and gel, respectively.

Substituting equation (6) into (5), the volume concentration of water in hydrogel ($\phi_s(t)$) as a function of the diffusion time (t) can be written as,

$$\phi_s(t) = v_s \bar{C}(t) = v_s \left[\frac{8}{\pi^2} \exp\left(-\frac{t\pi^2 D}{h^2} \right)(C_0 - C_f) + C_f \right] \tag{7}$$

Meanwhile, the diffusion coefficient (D) is governed by the Eyring equation as a function of temperature (T) [35],

$$D = D_0 \exp\left(-\Delta H / RT\right) \tag{8}$$

where D_0 is the initial diffusion coefficient and ΔH is the activation energy of the diffusion process.

Substituting equation (8) into (7), the volume concentration of the water in the hydrogel ($\phi_s(t)$) can be rewritten as,

$$\phi_s(t) = v_s \bar{C}(t) = v_s \left[\frac{8}{\pi^2} \exp\left(-\frac{t\pi^2 D_0}{h^2} \exp\left(-\frac{\Delta H}{RT} \right) \right)(C_0 - C_f) + C_f \right] \tag{9}$$

Substituting equations (7) and (9) into (4), the volume concentration of water in MC-water phase (ϕ_f) can be obtained as,

$$\phi_f = 1/\left(1+1/\left(\begin{array}{l} \dfrac{RT\alpha v_s}{M_{PW}\Delta\mu_{MW}} \left(\dfrac{8}{\pi^2} \exp\left(-\dfrac{t\pi^2 D_0}{h^2} \exp\left(-\dfrac{\Delta H}{RT} \right) \right)(C_0 - C_f) + C_f \right) + \\ \dfrac{RTA_2\alpha^2 v_s^2}{\Delta\mu_{MW}} \left(\dfrac{8}{\pi^2} \exp\left(-\dfrac{t\pi^2 D_0}{h^2} \exp\left(-\dfrac{\Delta H}{RT} \right) \right)(C_0 - C_f) + C_f \right)^2 \end{array} \right) \right) \tag{10}$$

Based on the phase transition theory [12], the stored strain ($\varepsilon_s = \varepsilon_{pre}\phi_f$) as a function of temperature can be written as,

$$\varepsilon_s = \varepsilon_{pre} / \left(1+1/ \left(\begin{array}{l} \dfrac{RT\alpha v_s}{M_{PW}\Delta\mu_{MW}} \left(\dfrac{8}{\pi^2} \exp\left(-\dfrac{t\pi^2 D_0}{h^2} \exp\left(-\dfrac{\Delta H}{RT} \right) \right) (C_0 - C_f) + C_f \right) + \\ \dfrac{RTA_2\alpha^2 v_s^2}{\Delta\mu_{MW}} \left(\dfrac{8}{\pi^2} \exp\left(-\dfrac{t\pi^2 D_0}{h^2} \exp\left(-\dfrac{\Delta H}{RT} \right) \right) (C_0 - C_f) + C_f \right)^2 \end{array} \right) \right) \quad (11)$$

where ε_{pre} is the pre-stored strain.

To verify the proposed model, a series of experimental data of the PAAm-MC DN hydrogels reported in Ref. [13] have been employed to compare with the analytical results obtained using equation (11). The parameters used in equation (11) are listed in Table 1, which were determined by the numerical analysis software 1stOpt. During the calculation process, the first step is to provide the basic value range of these parameters. Then the built-in universal global algorithm method in the 1stOpt software is applied to determine the values of parameters used in the simulation. The convergence tolerance is set as 10^{-10}, and the maximum iteration is set as 2000.

The obtained analytical and experimental results of the stored strains as a function of immersion time are plotted in Figure 2(a). At a constant cooling rate with the temperature decreased from 338 K to 283 K, the stored strain is gradually decreased from 0.27 to 0.03 with an increase in the immersion time from 0 s to 1500 s. The cooling-triggered SME enables the DN hydrogels to release the stored strain with a decrease in temperature. The water is gradually released from the DN hydrogel, and the MC component undergoes the hydrophobic transition and microphase separation at the lower temperature. Moreover, the divergences between the analytical and experimental results have been calculated based on correlation index (R^2), and the results are shown in Figure 2(b). A good agreement between the analytical results and

experimental data [13] has been achieved, where the error ratio is limited to the range from -6.88% to 13.18%.

Table 1. Values of fit parameters used in equation (11).

Parameters	$\frac{R\alpha v_s}{M_{PW}\Delta\mu_{MW}}$	$\frac{\pi^2 D_0}{h^2}$	ΔH	C_0	C_f	$\frac{A_2\alpha^2 v_s^2}{\Delta\mu_{MW}}$
Values	0.066	15.1	2265.1	0.4	4.3×10^{-3}	3.9×10^{-3}

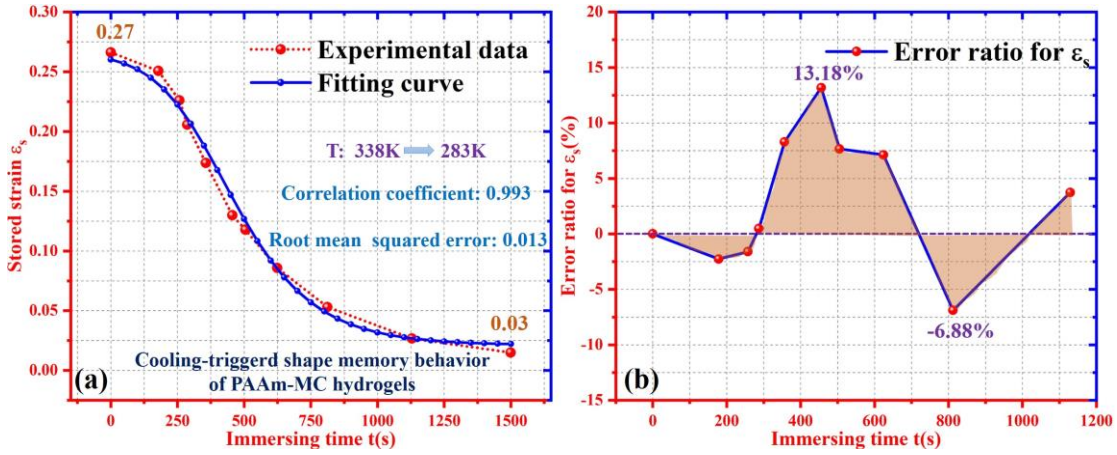

Figure 2. Analytical results and experimental data reported in Ref. [13] of stored strain as a function of immersion time of PAAm-MC DN hydrogel. (a) The stored strain as a function of immersion time. (b) Error ratio of stored strain.

To further investigate the effect of temperature on the shape memory DN hydrogels, the analytical results of stored strain as a function of immersion time have been plotted, at various temperatures of 250 K, 260 K, 270 K, 280 K and 290 K. As shown in Figure 3(a), the DN hydrogels take 1227 s, 1323 s, 1574 s, 2007 s and 2485 s, to complete their shape recovery processes at the temperatures of 250 K, 260 K, 270 K, 280 K and 290 K, respectively. With an increase in temperature, the hydrophobic transition of soft components becomes weakened, thus resulting in a decreased release rate of stored strains. Therefore, a longer immersion time is necessary for the stored

stain in DN hydrogel to be completely released. Moreover, the effect of temperature on the stored strain of DN hydrogels has been investigated based on equation (11), and the obtained results are shown in Figure 3(b). The analytical results reveal that the stored strain is decreased from 0.27 to 0.21 at 320 K, from 0.27 to 0.13 at 310 K and 0.27 to 0.04 at 300 K, respectively, at the same immersion time of 1500 s. Therefore, these analytical results prove that the DN hydrogel presents a cooling-triggered shape recovery.

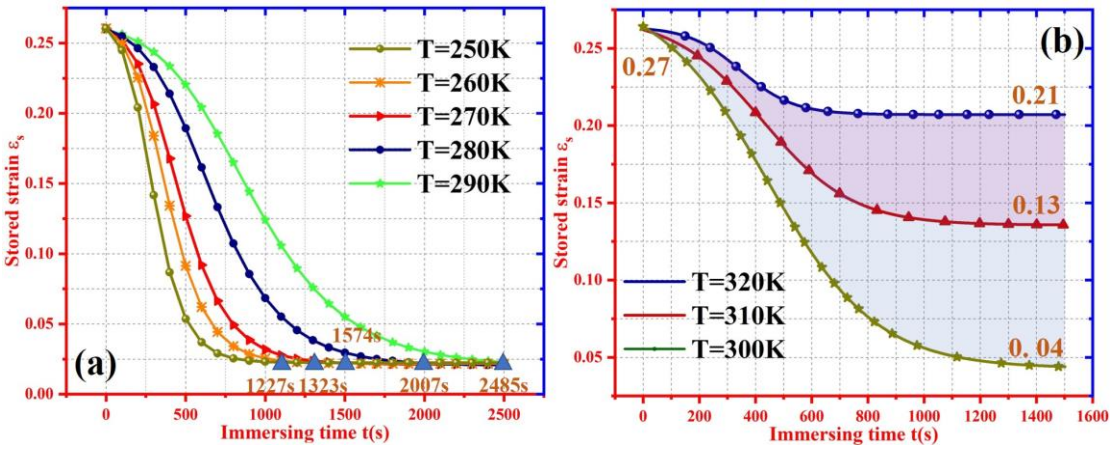

Figure 3. Analytical results of stored strain for shape memory DN hydrogel as a function of immersion time. (a) At various temperatures of 250 K, 260 K, 270 K, 280 K and 290 K. (b) At various temperatures of 300 K, 310 K and 320 K.

Furthermore, effects of diffusive thermodynamics parameters (i.e. diffusion length h and activation energy H) on the shape recovery behaviors have been investigated. Figure 4(a) plots the analytical results of stored strains as a function of immersion time at various diffusion lengths. With an increase in the diffusion length from 5 mm, 10 mm, 15 mm to 20 mm, the stored strains in the hydrogel are released at 307 s, 1273 s, 2567 s to 3894 s, respectively. The hydrogel takes a longer time to complete the shape recovery, when the diffusion length (h) is longer. On the other hand, the

effect of the diffusion activation energy on the stored strain has also been investigated based on equation (11), and the results are plotted in Figure 4(b). The analytical results reveal that the hydrogel takes times of 472 s, 598 s, 850 s, 1163 s and 1658 s to complete the shape recovery, when the diffusion activation energies are 1900 J/mol, 2000 J/mol, 2100 J/mol, 2200 J/mol and 2300 J/mol, respectively. The higher diffusion activation energy will promote the shape recovery, thus shortening the recovery time of hydrogel.

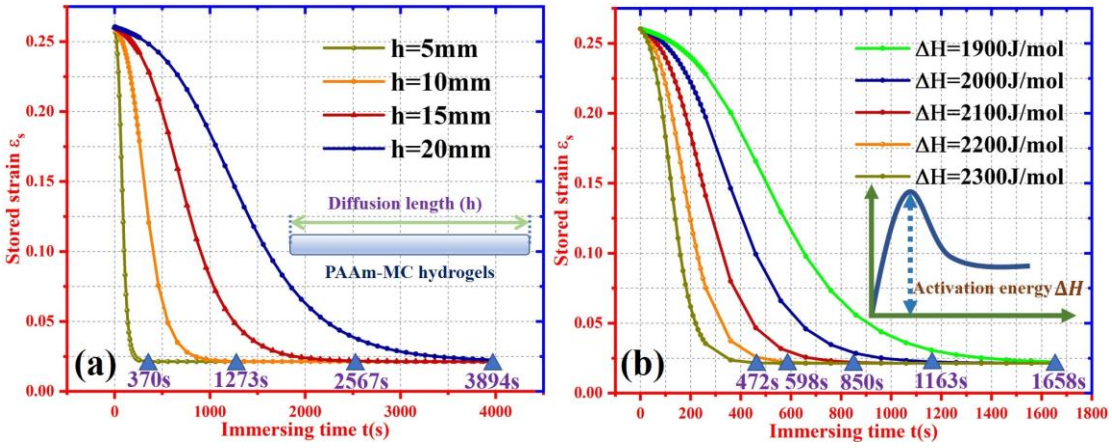

Figure 4. Analytical results of stored strain as a function of immersion time. (a) At various diffusion lengths of 5 mm, 10 mm, 15 mm and 20 mm. (b) At various activation energies of 1900 J/mol, 2000 J/mol, 2100 J/mol, 2200 J/mol and 2300 J/mol.

Finally, cooling-triggered multi-SME in PAAm-MC DN hydrogel was investigated, and the results are shown in Figure 5. A quadruple shape recovery behavior has been achieved by controlling the step-by-step cooling processes at 310 K, 305 K and 300 K. The DN hydrogel completes the first shape recovery at 310 K, whereas the stored strain is decreased from 0.27 to 0.13. Then, it completes the second shape recovery at 305 K, whereas the stored strain is decreased from 0.13 to 0.07. Finally, it completes the third shape recovery at 300 K, whereas the stored strain is decreased to 0.04.

These analytical results clearly show that the cooling-triggered multi-SME is highly programmable to achieve the multiple shape recovery behaviors. Therefore, the amplitude of cooling-triggered shape recovery, which is quite different from the conventional shape recovery of SMPs, appears strongly dependent on the hydrophobic transition and the associated microphase separation of MC component in PAAm-MC DN hydrogel. This provides a good methodology to design the cooling-triggered shape recovery behavior.

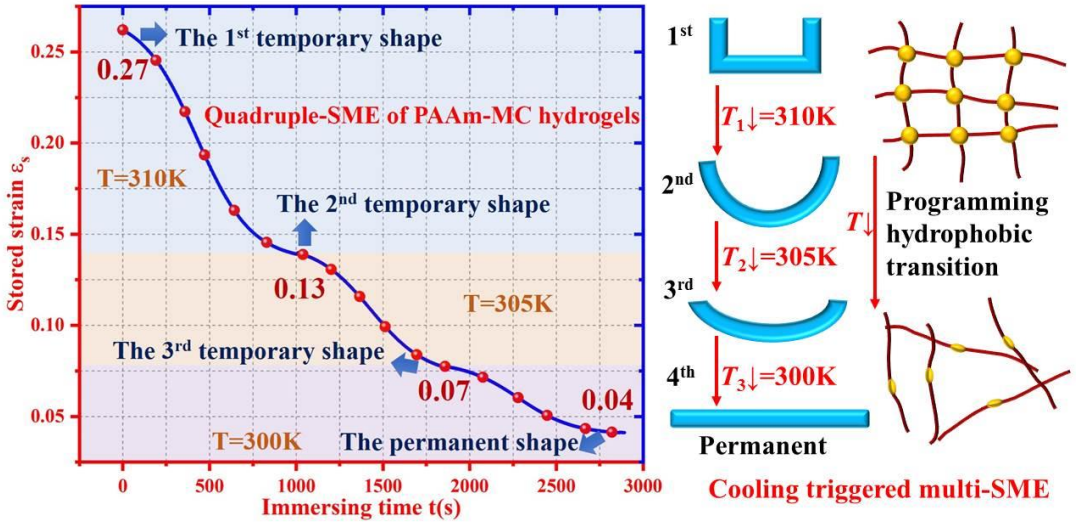

Figure 5. Analytical and experimental results [13] of stored strain as a function of immersion time for PAAm-MC DN hydrogel with quadruple-SME, which is achieved by programming cooling steps of 310 K, 305 K and 300 K.

3. Thermomechanical behavior of shape memory hydrogel

Thermomechanical behavior is an essential property of shape memory hydrogel [28]. According to the Obukhov model [32], the dependence of storage modulus (E) on volume concentration of the water (ϕ_s) in hydrogel can be written as,

$$E = 3(1-\phi_s)F_{el}^0 / a^3 N \tag{12}$$

where F_{el}^0 is the elastic energy, a^3 is the average volume of a hydrogel chain and N is the degree of crosslink.

According to the Flory-Huggins theory, the elastic energy (F_{el}^{0}) of a polymer chain can be expressed by [28,29],

$$F_{el}^{0}=\left(\lambda_0 R_0 / R\right)^2 k_b T \tag{13}$$

where R_0 and R are the root mean square end-to-end distances of the chains in gel and hydrogel, respectively, k_b is the Boltzmann constant and λ_0 is the swollen ratio.

The end-to-end distance of a hydrogel chain (R) can be described using the following equation [36]:

$$R=\mathrm{a}N^{v}\left(\phi_s /(1-\phi_s)\right)^{\frac{2v-1}{2(1-3v)}} \tag{14}$$

where a is a given constant and v is the exponent of excluded volume effect.

Assuming this process is a one-dimensional diffusion, the swollen ratio (λ_0) can be written as,

$$\lambda_0=1/\phi_s \tag{15}$$

By substituting equations (14) and (15) into (13), we can obtain the following relationship between the elastic energy and volume concentration of water,

$$F_{el}^{0}=\left(R_0 /\left(a\phi_s N^{v}\left(\phi_s /(1-\phi_s)\right)^{\frac{2v-1}{2(1-3v)}}\right)\right)^2 k_b T \tag{16}$$

Combining equations (12) and (16), the storage modulus (E) is given by,

$$E=\frac{3(1-\phi_s)k_b T}{a^3 N}\left(R_0 /\left(a\phi_s N^{v}\left(\phi_s /(1-\phi_s)\right)^{\frac{2v-1}{2(1-3v)}}\right)\right)^2 \tag{17}$$

To verify the proposed model, equation (17) is employed to predict the thermomechanical behavior of the shape memory hydrogel, whereas the effect of immersion time on the storage modulus has also been investigated. The analytical results in Figure 6 reveal that the storage modulus is gradually increased from 29.8

kPa, 38.4 kPa, 47.3 kPa, 56.7 kPa to 65.7 kPa with the temperature increased from 250 K, 260 K, 270 K, 280 K to 290 K, respectively. A distinct increase rate of 120% of thermomechanical storage modulus is obtained when the temperature is increased from 250 K to 290 K. These analytical results show that an increase in the temperature can cause the increase of storage modulus of shape memory hydrogel.

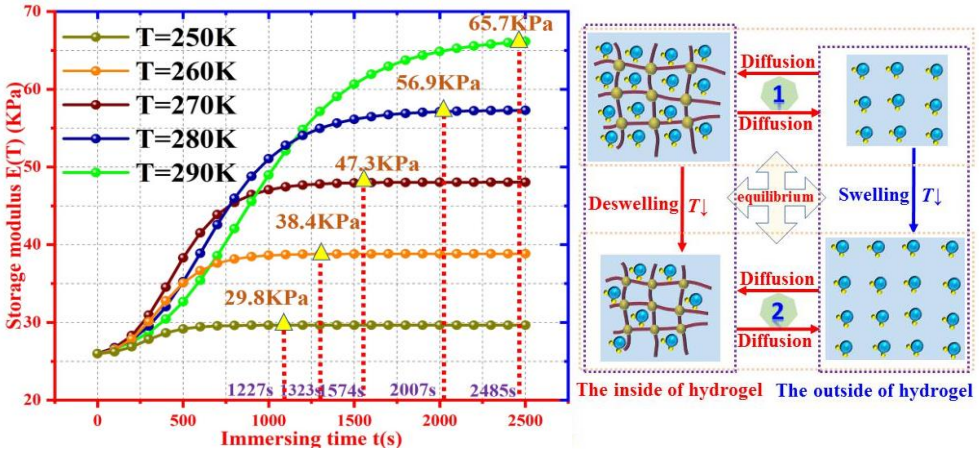

Figure 6. Analytical results of storage modulus as a function of immersing time for shape memory DN hydrogel at *T*=250 K, 260 K, 270 K, 280 K and 290 K.

On the other hand, the hydrogel takes a shorter recovery time to complete the shape recovery at a lower temperature. For example, it takes 1227 s, 1323 s, 1574 s, 2007 s to 2485 s to complete the shape recovery, when the hydrogel is heated to 250 K, 260 K, 270 K, 280 K and 290 K, respectively. For the cooling-triggered SME, the short recovery time is resulted from the low hydrophobic transition and microphase separation of soft component, which causes the hydrogel with a low value of storage modulus due to large volume concentration of water. Therefore, the storage modulus is decreased from 65.7 kPa to 29.8 kPa with the temperature decreased from 290 K to 250 K. Meanwhile, a high storage modulus of shape memory hydrogel is presented due to the increased hydrophobic transition and microphase separation at a high

temperature. Based on these analytical results, the thermomechanical behavior of shape memory hydrogel is originated from the cooling-triggered SME and is governed by the negatively thermodynamic toughening effect. With an increase in temperature, both the hydrophobic interaction and microphase separation are enhanced, which can increase the storage modulus of the hydrogel due to the low water concentration [37]. Meanwhile, the shape recovery time is increased due to the long diffusion time of large amount of water.

Furthermore, equation (17) is employed to predict the thermomechanical behavior of PAAm-MC DN hydrogel, and the applied constant parameters are k_b/a^3N=5.11, R_0=0.20 and ν=1.3 (based on the renormalized formula in Ref. [29]). The analytical and experimental results [13] of the storage moduli as a function of temperature are obtained and the results are shown in Figure 7. Figure 7(a) reveals that the storage modulus of the PAAm-MC DN hydrogel is gradually increased from 26 kPa to 101 kPa with an increase in temperature from 275 K to 327 K. A significant increase rate of 288% of storage modulus is obtained based on these analytical and experimental results. A negatively thermodynamic toughening effect is presented due to the cooling-triggered SME, which enables hydrophobic transition and microphase separation of MC component at a high temperature. An increase in storage modulus is therefore due to low water concentration (ϕ_s) based on the rubber elasticity theory [38]. Both the analytical and experimental results show that the storage moduli of the PAAm-MC hydrogel are increased with an increase in temperature. As shown in Figure 7(b), there are good agreements between the analytical and experimental

results, where the error ratio is limited to ±7.82%. These comparisons reveal that the analytical results obtained from the newly proposed model are suitable to characterize and predict the thermomechanical behaviors of the PAAm-MC DN hydrogel, which undergoes a negatively thermodynamic toughening.

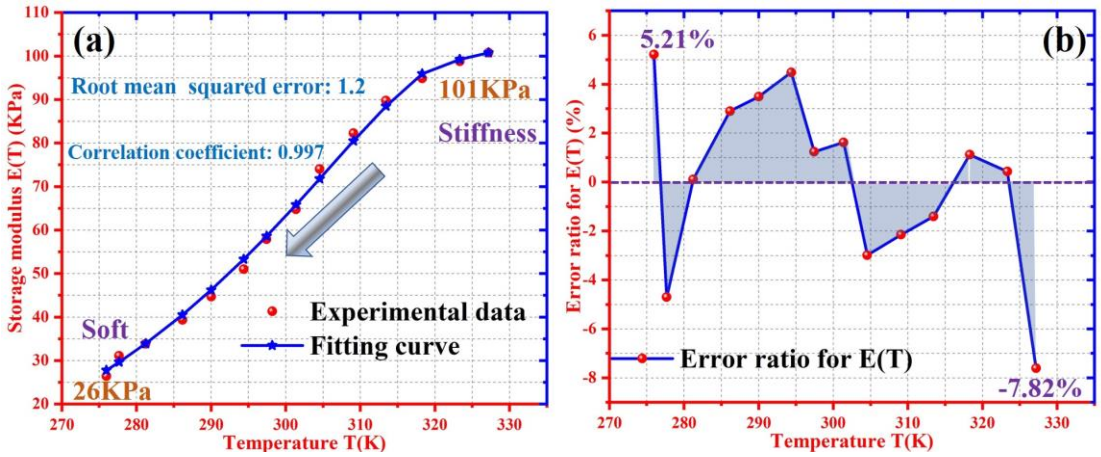

Figure 7. Analytical results and experimental data [13] of storage modulus of PAAm-MC DN hydrogel. (a) For the storage modulus as a function of temperature. (b) Error ratio of storage modulus.

4. Constitutive relationship of stress-stretching ratio

Furthermore, we derive the constitutive relationship between engineering stress (σ) and stretching ratio (λ_s) of the shape memory DN hydrogel in order to predict its mechanical behavior. Under the external stress, the stretching ratio (λ) can be written as,

$$\lambda=\lambda_0\lambda_s \tag{18}$$

Substituting equation (18) into (13), we can obtain,

$$F_{el}^0=\left(\lambda_0\lambda_s R_0/R\right)^2 k_bT \tag{19}$$

Meanwhile, the equation (16) can be then rewritten as,

$$F_{el}^0=\left(\lambda_s R_0/\left(a\phi_s(N^{'})^{\nu}\left(\phi_s/(1-\phi_s)\right)^{\frac{2\nu-1}{2(1-3\nu)}}\right)\right)^2 k_bT \tag{20}$$

According to the equation (17), the storage modulus (E) is given by,

$$E = \frac{3(1-\phi_s)k_bT}{a^3N}\left(\lambda_s R_0 / \left(a\phi_s (N^{'})^{\nu}\left(\phi_s / (1-\phi_s)\right)^{\frac{2\nu-1}{2(1-3\nu)}}\right)\right)^2 \tag{21}$$

Here, the Mooney-Rivin equation is employed to express the hyperelastic deformation of shape memory hydrogel [39], and the constitutive relationship between engineering stress (σ) and the stretching ratio (λ) can be obtained from,

$$\sigma = E\left(\lambda_s - \frac{1}{\lambda_s^{\,2}}\right) \tag{22}$$

Substituting equation (21) into (22), we can obtain the following expression,

$$\sigma = \frac{3(1-\phi_s)k_bT}{a^3N}\left(\lambda_s R_0 / \left(a\phi_s (N^{'})^{\nu}\left(\phi_s / (1-\phi_s)\right)^{\frac{2\nu-1}{2(1-3\nu)}}\right)\right)^2\left(\lambda_s - \frac{1}{\lambda_s^{\,2}}\right) \tag{23}$$

To verify the proposed model of equation (23), the effects of temperature and water volume concentration on the engineering stress have been investigated, and the obtained results are shown in Figure 8. Figure 8(a) shows the effect of temperature on the engineering stress. The analytical results reveal that the engineering stress is gradually increased from 19.27 kPa, 57.8 kPa, 96.4 kPa, 134.9 kPa to 173.4 kPa, at the temperature of 290 K, 300 K, 310 K, 320 K and 330 K, respectively. A significant increase rate of 800% of engineering stress is obtained when the temperature is increased from 290 K to 330 K.

On the other hand, the effect of water concentration on the engineering stress has also been studied, and the results are shown in Figure 8(b). It is revealed that the engineering stress is gradually increased from 33.6 kPa, 44.8 kPa, 56.1 kPa, 67.2 kPa to 78.4 kPa with a decrease in volume concentration of water from 95.5%, 92.5%, 90.0%, 87.5% to 85.0%. An increase rate of 134% of engineering stress is achieved,

whereas the ϕ_s is decreased from 95.5% to 85.0%. The large engineering stress is resulted from the low water concentration (ϕ_s) based on the rubber elasticity theory [38].

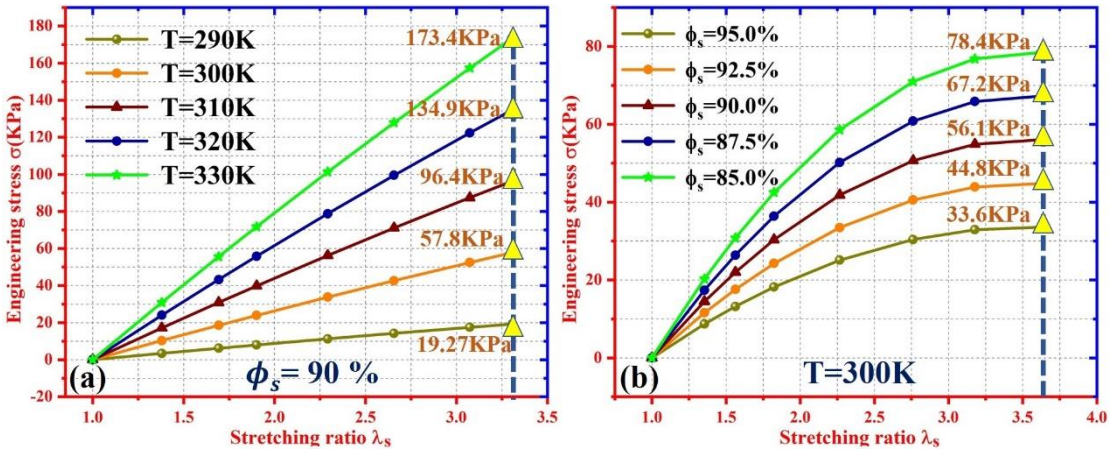

Figure 8. Analytical results of engineering stress as a function of stretching ratio. (a) At *T*=290 K, 300 K, 310 K, 320 K and 330 K. (b) At ϕ_s =85%, 87.5%, 90%, 92.5% and 95%.

Furthermore, two groups of experimental data [13] of PAAm-MC DN hydrogels have been used to verify the analytical results obtained using the proposed model of equation (23). Figure 9 compares the analytical and experimental results, and it is revealed that the proposed model well predicts the experimental results. By increasing the temperature from 293 K to 338 K, the engineering stress (σ) is increased from 24.7 kPa to 184 kPa at the same stretching ratio (λ) of 3.31, whereas an increase rate of 645% of engineering stress is achieved. A negatively thermodynamic toughening is also confirmed from both the analytical and experimental results of engineering stress (σ) as a function of the stretching ratio (λ). The hydrogel shows a higher engineering stress (σ) at a higher temperature. The effectiveness of model is verified by the experimental results of engineering stress (σ) as a function of stretching ratio of PAAm-MC DN hydrogel reported in literature [13].

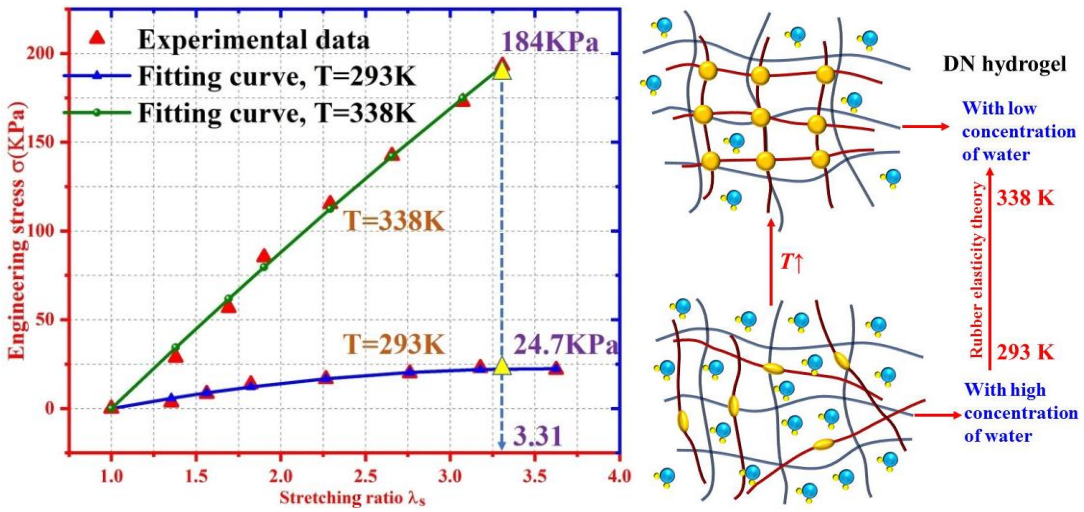

Figure 9. Analytical and experimental results [13] of engineering stress (σ) as a function of stretching ratio (λ) of PAAm-MC DN hydrogel at T=293 K and 338 K.

5. Conclusions

In this study, we proposed a thermodynamic model to understand the cooling-triggered multi-SME and microphase separation in the shape memory DN hydrogel. The proposed constitutive framework provides an effectively theoretical approach to characterize the negatively thermodynamic toughening effect, thermomechanical shape recovery behavior and mechanical properties. The negatively thermodynamic toughening is mainly due to hydrophobic interaction and microphase separation in the DN hydrogels. Our analysis reveals that both the thermomechanical storage modulus and engineering stress have been significantly enhanced up to 800% and 645%, with an increase in the temperature of 40ºC and 45ºC, respectively. A designable and cooling-triggered dual- and quadruple-SME is achieved and predicted by the proposed model for the DN hydrogel. Finally, the effectiveness of model was well verified using the experimental data of PAAm-MC DN hydrogel reported in literature.

Acknowledgements

This work was financially supported by the National Natural Science Foundation of China (NSFC) under Grant No. 11725208 and International Exchange Grant (IEC/NSFC/201078) through Royal Society UK and NFSC.

References

[1] Lendlein A, Jiang H Y, Jünger O and Langer R 2005 Light-induced shape-memory polymers *Nature* **434** 879–82

[2] Mather P T, Luo X F and Ingrid A 2007 Rousseau shape memory polymer research *Annu. Rev. Mater. Res.* **39** 445–71

[3] Xie T 2011 Recent advances in shape memory polymer *Polymer* **52** 4985–5000

[4] Hu J L, Zhu Y, Huang H H and Lu J 2012 Recent advances in shape–memory polymers: structure, mechanism, functionality, modeling and applications *Prog. Polym. Sci.* **37** 1720–63

[5] Meng H and Lia G Q 2013 A review of stimuli-responsive shape memory polymer composites *Polymer* **54** 2199–221

[6] Sun L, Huang W M, Ding Z, Zhao Y, Wang C C, Purnawali H and Tang C 2012 Stimulus-responsive shape memory materials: a review *Mater. Des.* **33** 577–640

[7] Hoeher R, Raidt T, Katzenberg F and Tiller J C 2016 Heating rate sensitive multi-shape memory polypropylene: a predictive material *ACS Appl. Mater. Inter.* **8** 13684–7

[8] Zhang H and Zhao Y 2013 Polymers with dual light-triggered functions of shape memory and healing using gold nanoparticles *ACS Appl. Mater. Inter.* **5** 13069–75

[9] Huang W M, Zhao Y, Wang C C, Ding Z, Hurnawali H, Tang C and Zhang J L 2012 Thermo/chemo-responsive shape memory effect in polymers: a sketch of working mechanisms, fundamentals and optimization *J. Polym. Res.* **19** 9952

[10] Alteheld A, Feng Y K, Kelch S and Lendlein A 2005 Biodegradable, amorphous

copolyester-urethane networks having shape-memory properties *Angew. Chem. Int. Edit.* **44** 1188-92

[11] Liu Y P, Gall K, Dunn M L, Greenberg A R and Diani J 2006 Thermomechanics of shape memory polymers: uniaxial experiments and constitutive modeling *Int. J. Plasticity* **22** 279-313

[12] Wang C C, Huang W M, Ding Z, Zhao Y and Hurnawali H. 2012 Cooling-/water-responsive shape memory hybrids *Compos. Sci. Technol.* **72** 1178-82

[13] Hu X, Zhang D and Sheiko S S 2018 Cooling-triggered shapeshifting hydrogels with multi-shape memory performance *Adv. Mater.* **30** 1707461

[14] Hirrien M, Chevillard C, Desbrieres J, Axelos M A V and Rinaudo M 1998 Thermogelation of methylcelluloses: new evidence for understanding the gelation mechanism *Polymer* **39** 6251-9

[15] Kobayashi K, Huang C I and Lodge T P 1999 Thermoreversible gelation of aqueous methylcellulose solutions *Macromolecules* **32** 7070-7

[16] Desbrieres J, Hirrien M and Ross-Murphy S B 2000 Thermogelation of methylcellulose: rheological considerations *Polymer* **41** 2451-61

[17] Ge Q, Luo X, Iversen C B, Mather P T, Dunn M L and Qi H J 2013 Mechanisms of triple-shape polymeric composites due to dual thermal transitions *Soft Matter* **9** 2212–23

[18] Zhao Q, Qi H J and Xie T 2015 Recent progress in shape memory polymer: new behavior, enabling materials, and mechanistic understanding *Prog. Polym. Sci.*

49–50 79-120

[19]Meng Y, Jiang J S and Anthamatten M 2016 Body temperature triggered shape–memory polymers with high elastic energy storage capacity *J. Polym. Sci. Part B: Polym. Phys.* **54** 1397-404

[20] Chan B Q Y, Low Z W K, Heng S J W, Chan S Y, Owh C and Loh X J 2016 Recent advances in shape memory soft materials for biomedical applications *ACS Appl. Mater. Inter.* **8** 10070-87

[21] Chester S A and Anand L 2010 A coupled theory of fluid permeation and large deformations for elastomeric materials *J. Mech. Phys. Solids* **58** 1879–906

[22]Chester S A and Anand L 2011 A thermo-mechanically coupled theory for fluid permeation in elastomeric materials: application to thermally responsive gels *J. Mech. Phys. Solids* **59** 1978–2006

[23]Chester S A, Di Leo C V. and Anand L 2015 A finite element implementation of a coupled diffusion-deformation theory for elastomeric gels *Int. J. Solids Struct.* **52** 1–18

[24] Liu Y, Zhang H and Zheng Y 2016 A micromechanically based constitutive model for the inelastic and swelling behaviors in double network hydrogels *J. Appl. Mech. Trans. ASME* **83** 021008

[25] Xiao R, Mai T T, Urayama K, Gong J P and Qu S 2021 Micromechanical modeling of the multi-axial deformation behavior in double network hydrogels *Int. J. Plast.* **137** 102901

[26] Mao Y, Lin S, Zhao X and Anand L 2017 A large deformation viscoelastic model for double-network hydrogels *J. Mech. Phys. Solids* **100** 103–30

[27] Xing Z, Lu H and Fu Y Q 2021 Local conservation law of rubber elasticity in hydrogel networks undergoing microphase separation and toughening *Polymer* **222** 123656

[28] P. J. Flory 1953 *Principles of polymer chemistry* (Ithaca, NY: Cornell University Press)

[29] Gennes P G 1979 Scaling concepts in polymer physics (Ithaca, NY: Cornell University Press)

[30]Chen S, Hu J and Zhuo H 2011 Study on the moisture absorption of pyridine containing polyurethane for moisture-responsive shape memory effects *J. Mater. Sci.* **46** 6581–8

[31] Shi X, Soule D, Mao Y, Yakacki C, Lu H and Yu K 2020 A multiscale chemomechanics theory for the solvent-Assisted recycling of covalent adaptable network polymers *J. Mech. Phys. Solids* **138** 103918

[32] Obukhov S P, Rubinstein M and Colby R H 1994 Network modulus and superelasticity *Macromolecules* **27** 3191–8

[33] Xing Z Y, Lu H B, Sun A S, Fu Y Qing, Shahzad M W and Xu B B 2021 Understanding complex dynamics of interfacial reconstruction in polyampholyte hydrogels undergoing mechano-chemo-electrotaxis coupling *J. Phys. D: Appl. Phys.* **54** 085301

[34]Hong K, Rastogi A and Strobl G 2004 A model treating tensile deformation of

semicrystalline polymers: quasi-static stress-strain relationship and viscous stress determined for a sample of polyethylene *Macromolecules* **37** 10165–73

[35] Vrentas J S and Duda J L 1977 Solvent and temperature effects on diffusion in polymer–solvent systems *J. Appl. Polym. Sci.* **21** 1715–28

[36] Wang X, Lu H, Wu N, Hui D and Fu Y 2019 Unraveling bio-inspired pre-swollen effects of tetra-polyethylene glycol double network hydrogels with ultra-stretchable yielding strain *Smart Mater. Struct.* **28** 035005

[37] Murakawa K, King D R, Sun T L, Guo H, Kurokaw T and Gong J P 2019 Polyelectrolyte complexation via viscoelastic phase separation results in tough and self-recovering porous hydrogels *J. Mater. Chem. B* **7** 5296–305

[38] Xing Z Y, Lu H B, Hossain M, Fu Y Q, Leng J S and Du S Y 2020 Cooperative dynamics of heuristic swelling and inhibitive micellization in double-network hydrogels by ionic dissociation of polyelectrolyte *Polymer* **186** 122039

[39] Lu H, Wang X, Shi X, Yu K and Fu Y Q 2018 A phenomenological model for dynamic response of double-network hydrogel composite undergoing transient transition *Compos. Part B Eng.* **151** 148–53